THE JOURNAL OF PHYSICAL CHEMISTRY LETTERS
A JOURNAL OF THE AMERICAN CHEMICAL SOCIETY

pubs.acs.org/JPCL Letter

Gas-Phase Formation of Silicon Dicarbide (c-SiC_2): A Key Cyclic Precursor to Silicon Carbide Grains in Space

Shane J. Goettl, Iakov A. Medvedkov, Zhenghai Yang, Surajit Metya, Márcio O. Alves, Breno R. L. Galvão,* and Ralf I. Kaiser*

Cite This: *J. Phys. Chem. Lett.* 2026, 17, 9334−9340 Read Online

ACCESS | Metrics & More | Article Recommendations | Supporting Information

ABSTRACT: Complex organosilicon molecules are pervasive in interstellar environments, yet the mechanisms governing their formation—particularly the initial silicon−carbon bond coupling—remain largely unexplored. Such processes initiate reaction networks that generate precursors to silicon carbide (SiC) dust grains, which enable galactic-cosmic-ray−driven synthesis of complex organic molecules, including amino acids and sugars, in deep space. Here, we combine crossed molecular beam experiments with high-level computations to show that a postulated precursor to SiC grains—cyclic silicon dicarbide (c-SiC_2)—forms via reaction of the simplest silicon-bearing radical, silylidyne (SiH), with dicarbon (C_2). This barrierless, exoergic reaction links simple silicon- and carbon-bearing molecular reservoirs, initiating molecular mass growth even under the low-temperature conditions of dense molecular clouds such as G+0.693−0.027, where c-SiC_2 has recently been detected. Organosilicon species such as silicon dicarbide thus drive exoergic reaction networks culminating in SiC grain formation, bridging the gap between simple molecules and interstellar SiC dust.

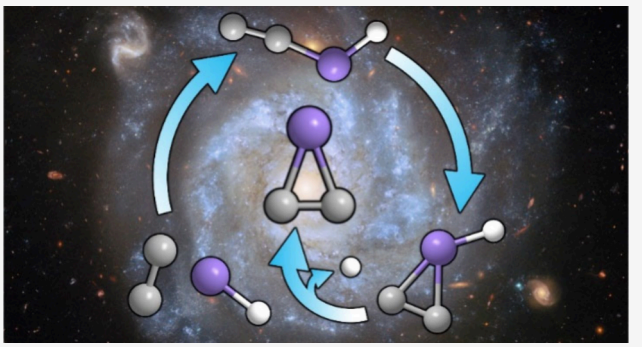

Since the detection of the cyclic, C_{2v}-symmetric silicon dicarbide molecule (c-SiC_2, X^1A_1) in the circumstellar envelope of the asymptotic giant branch (AGB) carbon star IRC+10216 by Thaddeus et al. in 1984,[1] silicon−carbon clusters have been recognized as fundamental molecular building blocks of silicon carbide (SiC) grains in space. These grains are observed via their characteristic 11.3 μm (885 cm^{-1}) emission band[2] and in primitive meteorites such as Murray[3] and Murchison.[4] Alongside refractory sulfide,[5] silicate,[6] and carbonaceous grains,[7] nanometer-scale particles containing silicon carbide cores are a major component of the interstellar medium (ISM).[8] They are thought to form primarily in supernova explosions and in the circumstellar envelopes of evolved stars such as asymptotic giant branch (AGB) carbon stars.[9−11]

Formation of SiC grains in circumstellar environments is predicted to initiate through silicon−carbon bond formation in hot inner envelopes. Proposed reactions involve silicon (Si) atoms with acetylene (C_2H_2)[12] or ethynyl radicals (C_2H),[13] where reactive species such as Si(^{3}P) and silylidyne radicals (SiH, $X^2\Pi$) are generated in shocks at temperatures up to 3,500 K.[13−15] Products are transported outward by stellar winds to cooler regions, where ultraviolet irradiation can photodissociate carbon−hydrogen and silicon−hydrogen bonds, yielding pure silicon−carbon clusters.[13] Gas-phase models further suggest that sequential molecular growth from species such as silicon carbide (SiC) and 1,3,5-trisiladehydrobenzene (Si_3C_3) can produce larger clusters.[16]

However, silicon carbide grain formation in stellar outflows occurs on time scales of 10^9 yr,[17,18] whereas interstellar grain destruction due to sputtering, shocks, and collisions occur on time scales of 10^8 yr.[19−23] This imbalance indicates that additional formation routes operate under interstellar conditions, likely involving bottom-up molecular growth in low-temperature molecular clouds.[24−26] Support for this scenario comes from the recent detection of silicon dicarbide (c-SiC_2)—a proposed precursor of silicon carbide grains[27]—in the molecular cloud G+0.693−0.027.[28] As the first silicon−carbon ring molecule observed in both circumstellar and interstellar media, c-SiC_2 has attracted considerable interest and has been used to probe physical conditions in stellar atmospheres via the Merrill−Sanford band system ($\tilde{A}^1B_2$-$\tilde{X}^1A_1$).[29−31] Its presence emphasizes the importance of considering bottom-up molecular growth of silicon−carbon

Received: May 19, 2026
Revised: June 11, 2026
Accepted: June 16, 2026
Published: June 29, 2026

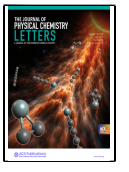

https://doi.org/10.1021/acs.jpclett.6c01640
J. Phys. Chem. Lett. 2026, 17, 9334−9340

clusters in cold interstellar environments (10 K), in addition to high-temperature circumstellar processes.[32−35]

Nevertheless, mechanistic studies of silicon dicarbide (c-SiC_2) formation under gas-phase conditions remain scarce. A proposed pathway involving silicon atoms reacting with acetylene followed by molecular hydrogen loss[36,37] has not been experimentally confirmed.[38] Crossed molecular beam experiments have shown the formation of silacyclopropenylidene (c-SiC_2H_2), a hydrogenated analogue, via the reaction of silylidyne radicals (SiH) with acetylene (C_2H_2),[39] but subsequent photodissociation steps would be required to yield c-SiC_2. Such multistep sequences are slower than a bimolecular reaction capable of forming c-SiC_2 in a single collision event at cold interstellar temperatures.

Herein, we report the gas-phase formation of cyclic silicon dicarbide (c-SiC_2, X^1A_1) via the reaction of dicarbon (C_2, $X^1\Sigma_g^+/a^3\Pi_u$) with silylidyne radicals (SiH, $X^2\Pi$) exploiting crossed molecular beams combined with electronic structure calculations. The silylidyne radical adds to dicarbon without an entrance barrier, forming a silylidyne-ethynyl intermediate that undergoes cyclization and hydrogen atom ejection to yield c-SiC_2. Cyclic silicon dicarbide is a three-membered ring 220 kJ mol^{-1} more stable than the linear isomer, contrasting with its isovalent counterpart tricarbon (C_3, $X^1\Sigma_g^+$), whose linear ground state lies 84 kJ mol^{-1} below the cyclic form (Figure 1).

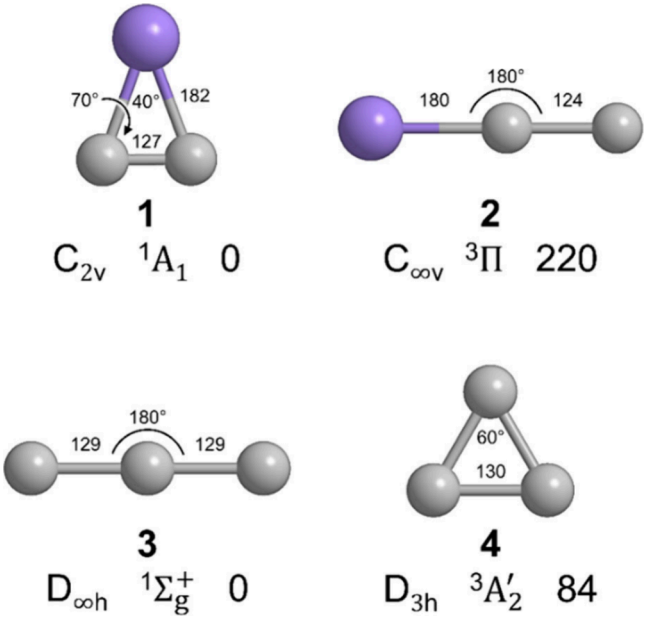

Figure 1. Geometries, point groups, electronic states, and relative energies (kJ mol^{-1}) of silicon dicarbide (SiC_2) and its isovalent counterpart, tricarbon (C_3), in their cyclic and linear forms.

The cyclic structure of tricarbon is a triplet with an equilateral triangle shape (C−C ∼ 130 pm), whereas c-SiC_2 is a singlet with elongated Si−C bonds (∼182 pm) and C_{2v} symmetry (Figure 1). The latter exhibits polytopic character, partial ionic bonding between silicon and the dicarbon moiety, and a hindered "pinwheel" rotation.[40−44] Since this dicarbon−silylidyne reaction is barrierless, exoergic, and all intermediates and transition states lie below the reactants, it proceeds efficiently in cold molecular clouds such as G+0.693−0.027. Dicarbon is ubiquitous in space,[45−49] while silylidyne has been inferred toward Orion KL[50] and can form via photodissociation or cosmic-ray degradation of silane (SiH_4). Small organosilicon molecules like c-SiC_2 can therefore initiate an exoergic chemistry leading to silicon-carbide grains, linking simple molecular species to interstellar dust and providing fundamental insight into the galactic life cycle of silicon carbide.

The crossed molecular beams technique was utilized to explore the bimolecular reaction of dicarbon (C_2, $X^1\Sigma_g^+/a^3\Pi_u$) with the silylidyne radical (SiH, $X^2\Pi$) in the gas phase under single-collision conditions. Details on the experimental procedure and the generation of the transient species in the supersonic beams are compiled in the Supporting Information. In short, a dicarbon beam was generated via laser ablation of a graphite rod and seeding of the ablated species in helium carrier gas, while the silylidyne radical beam was produced via photodissociation of disilane (Si_2H_6) seeded in helium carrier gas at a fraction of 0.5%. Both the dicarbon and silylidyne radical beams crossed perpendicularly at a collision energy of 42.9 ± 1.8 kJ mol^{-1}. Reactively scattered products were collected at different angles within the plane of the reactant beams and analyzed using time-of-flight (TOF) mass spectrometry. TOF spectra were collected at mass-to-charge ratios (m/z) of 54 ($SiC_2H_2^+$, $^{29}SiC_2H^+$, $Si^{13}CCH^+$), 53 (SiC_2H^+, $^{29}SiC_2^+$, $Si^{13}CC^+$), and 52 (SiC_2^+) at the center-of-mass (CM) angle (Θ_{CM}) of 47.8 ± 1.1° with respect to the dicarbon beam. No products were observed at m/z = 54 and 53, which reveals that any silyl radicals (SiH_3) or silane (SiH_4)—if generated from photodissociation of disilane—either do not react or do not lead to interfering scattering signal with dicarbon under our experimental conditions. Signal obtained at m/z = 52 could originate from three different sources. First, the reaction of dicarbon with the silylidyne radical results in the formation of SiC_2 along with atomic hydrogen (**1**). Second, the reaction of dicarbon with disilane, which is also present in the silylidyne beam, results in the formation of $Si_2C_2H_4$ products plus molecular hydrogen (**2**) as verified experimentally (Supporting Information). The $Si_2C_2H_4$ products may fragment in the electron impact ionizer to SiC_2^+ granting detectable signal at m/z = 52. Finally, since the laser ablation process also generates tricarbon (C_3) in addition to dicarbon, the reaction of tricarbon with silylidyne radicals was previously shown to yield SiC_3 molecules through atomic hydrogen loss (**3**).[51] As for the dicarbon−disilane case, the SiC_3 products fragment in the ionizer to signal at m/z = 52. Reactions of tricarbon with disilane, silane, silyl, and silylene—if present in the reactant beam—were found not to occur (Supporting Information).

TOFs were collected at m/z = 52 in steps of 3° to 5° in the angular range of 27° to 65° with respect to the dicarbon beam (0°) (Figure 2b). The TOFs were quite narrow featuring widths of about 200 μs. The integrated intensity of the TOFs at each angle was normalized to the TOF collected near the Θ_{CM} of 47.8° resulting in the laboratory angular distribution (LAD) (Figure 2a). The LAD shows a clear peak at about 46° with lower angles decreasing in intensity and higher angles dipping slightly before increasing again. Additional information on this system was acquired by converting the laboratory data into the CM frame of reference.[52]

$$C_2(24\ \text{amu}) + SiH(29\ \text{amu}) \rightarrow SiC_2(52\ \text{amu}) + H(1\ \text{amu}) \quad (1)$$

$$C_2(24\ \text{amu}) + Si_2H_6(62\ \text{amu}) \rightarrow Si_2C_2H_4(84\ \text{amu}) + H_2(2\ \text{amu}) \quad (2)$$

https://doi.org/10.1021/acs.jpclett.6c01640
J. Phys. Chem. Lett. 2026, 17, 9334−9340

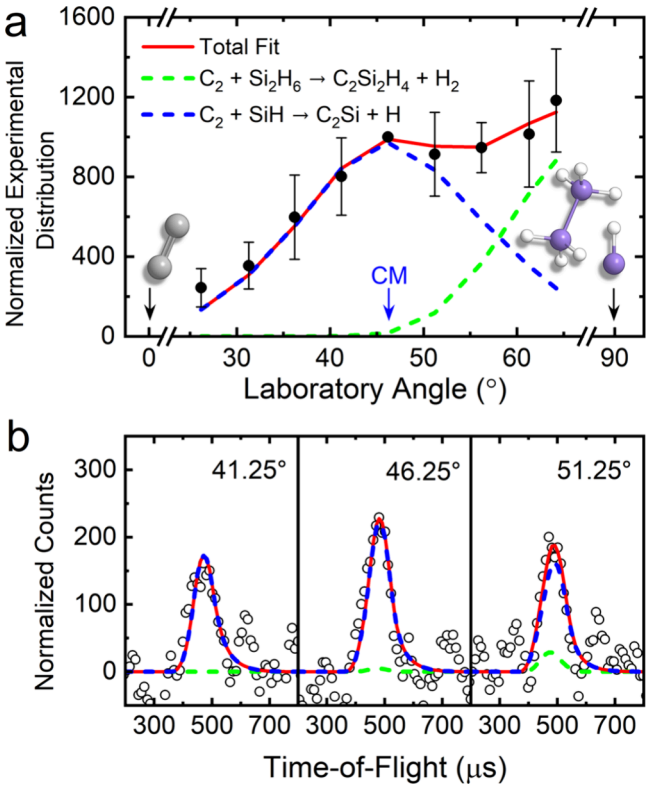

Figure 2. Laboratory angular distribution (a) and time-of-flight (TOF) spectra (b) recorded at mass-to-charge (m/z) = 52 for the reaction of dicarbon (C_2) with the silylidyne radical (SiH). CM represents the center-of-mass angle, and 0° and 90° define the directions of the dicarbon and silylidyne beams, respectively. The black circles depict the data, green lines show the dicarbon−disilane reaction fits, blue lines show the dicarbon−silylidyne fits, and red lines show the total fits (the sum of the blue and green curves).

$$C_3(36\ \text{amu}) + SiH(29\ \text{amu}) \rightarrow SiC_3(64\ \text{amu}) + H(1\ \text{amu}) \quad (3)$$

The conversion of the laboratory data into the CM reference frame generates a translational energy flux distribution ($P(E_T)$) and an angular flux distribution ($T(\theta)$). These functions are exploited to obtain the flux contour map (Figure 3). The TOFs and LAD at m/z = 52 cannot be fit with a single channel of only reactions **1**, **2**, or **3**. Two channels incorporating reactions **1** and **2** are required to fit the experimental data. Here, the reaction of dicarbon with silylidyne forming SiC_2 products coupled with atomic hydrogen loss (**1**) is represented by the blue curve in Figure 2a; the fragmentation of the $Si_2C_2H_4$ products generated from the dicarbon−disilane reaction plus molecular hydrogen (**2**) is displayed by the green curve (Supporting Information). The CM functions for the dicarbon−silylidyne system are shown in Figure 3. First, the $P(E_T)$ exhibits a maximum translational energy (E_{max}) at 440 ± 63 kJ mol^{-1} (Figure 3a). The conservation of energy dictates that the reaction energy ($\Delta_r G$) can be recovered with $\Delta_r G = E_C - E_{max}$ for those products without internal energy, i.e. the maximum kinetic energy release (E_{max}), where E_C is the reaction collision energy. Using E_C = 42.9 ± 1.8 kJ mol^{-1}, the reaction energy is determined to be −397 ± 65 kJ mol^{-1}. Furthermore, the distribution peaks near zero, which is indicative of a loose exit transition state with little electron rearrangement once the SiC_2H reaction intermediate decomposes unimolecularly to SiC_2 and atomic hydrogen.[53] Next, the $T(\theta)$ features symmetry about 90° indicating that the reaction of dicarbon with silylidyne is indirect (Figure 3b). The greater intensity at the poles with a dip at 90° suggests geometric constraints such that the hydrogen atom ejection occurs perpendicular to the total angular momentum vector and within the rotational plane of the decomposing complex. This finding coincides with the LAD analysis, where the experimental data would feature a symmetric distribution about the Θ_{CM} without the contribution from the dicarbon−disilane reaction (Figure 2a). Lastly, the flux contour map (Figure 3c) denotes the product of the $P(E_T)$ and $T(\theta)$, providing a two-dimensional image of the overall reaction outcome. The CM functions and analysis for the dicarbon−disilane system (**2**) are in the Supporting Information.

With the formation of SiC_2 product(s) coupled with atomic hydrogen loss through the reaction of dicarbon with the silylidyne radical experimentally established, additional mech-

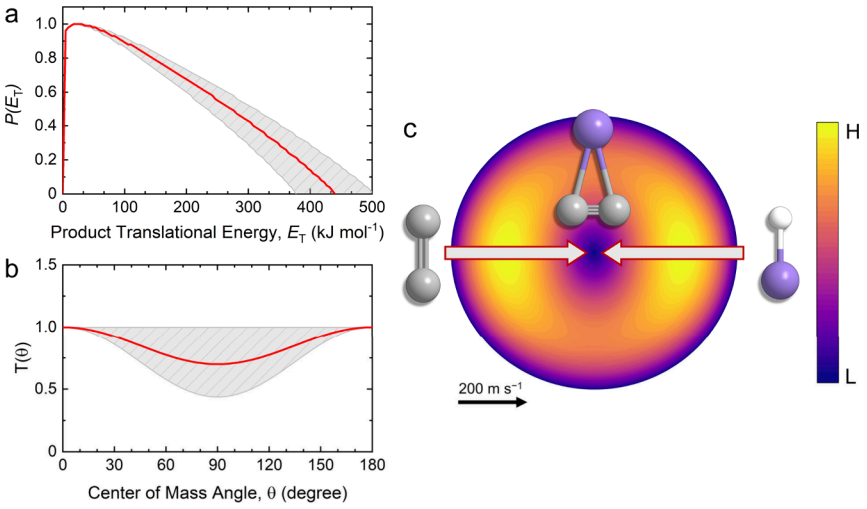

Figure 3. Center-of-mass product translational energy (a) and angular (b) flux distributions as well as the associated flux contour map (c) leading to the formation of SiC_2 isomer(s) in the reaction of dicarbon (C_2) with the silylidyne radical (SiH). Red lines define the best-fit functions while shaded areas provide the error limits. The flux contour map represents the intensity of the reactively scattered products as a function of product velocity (u) and scattering angle (θ), and the color bar indicates flux gradient from low (L) to high (H) intensity.

https://doi.org/10.1021/acs.jpclett.6c01640
J. Phys. Chem. Lett. 2026, 17, 9334−9340

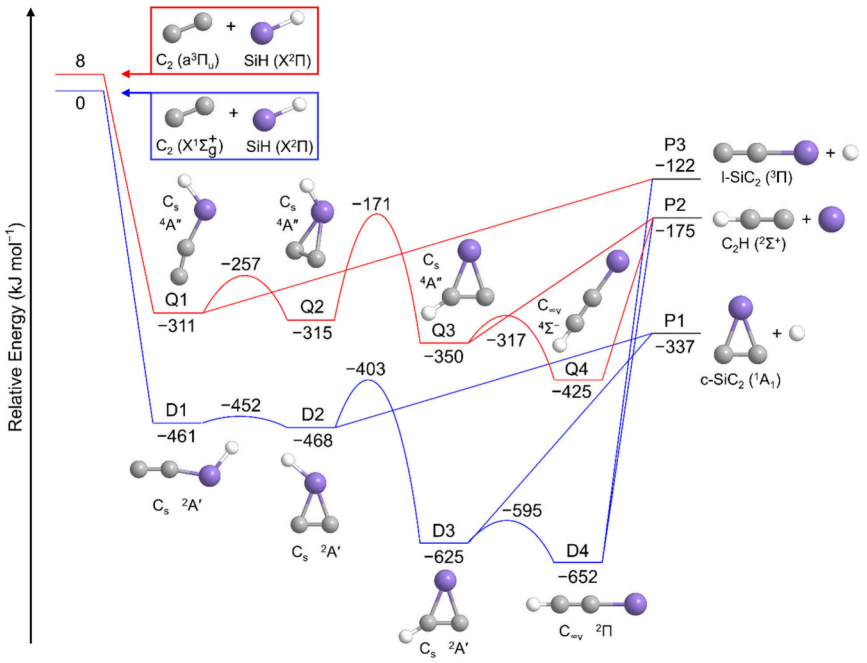

Figure 4. Schematic potential energy surfaces (PES) for the reactions of dicarbon (C_2) in its $X^1\Sigma_g^+$ (blue lines) and $a^3\Pi_u$ (red lines) states with the silylidyne radical (SiH) calculated at the CCSD(T)-F12/aug-cc-pV(Q+d)Z//B2PLYP-D3/def2-TZVP + ZPE(B2PLYP-D3/def2-TZVP) level. Relative energies are given in kJ mol^{-1}, and electronic states are provided for reactants, intermediates, and products.

anistic insights and product isomer confirmation were obtained by combining the experiments with high-level electronic structure calculations. The structures of the reactants, intermediates, and products as well as the energetics of all species are compiled on the potential energy surface (PES) (Figure 4) calculated at the CCSD(T)-F12/aug-cc-pV(Q+d)Z//B2PLYP-D3/def2-TZVP + ZPE(B2PLYP-D3/def2-TZVP) level of theory[54−62] with accuracies of ± 4 kJ mol^{-1}. There are two silicon dicarbide isomers—cyclic (c-SiC_2, X^1A_1, **P1**) and linear (l-SiC_2, $X^3\Pi$, **P3**)—resulting from atomic hydrogen loss which lie 337 kJ mol^{-1} and 122 kJ mol^{-1}, respectively, below the separated reactants. The experimentally derived reaction energy of −397 ± 65 kJ mol^{-1} matches the calculated value for the cyclic isomer (**P1**, −337 kJ mol^{-1}); all other product reaction energies lie outside the experimental error bars. This finding reveals the formation of at least **P1** from the reaction of dicarbon with the silylidyne radical; however, **P2** and **P3** cannot be discounted as their kinetic energy release may be cloaked within the lower energy portion of the $P(E_T)$ (Figure 3a). Note that background counts from (in)elastic scattering of ^{13}CC from the dicarbon beam at m/z = 25 were too high to observe **P2**.

It is important to note that the dicarbon beam contained both ground singlet state ($X^1\Sigma_g^+$) and excited triplet state ($a^3\Pi_u$) dicarbon molecules during the experiments (Supporting Information);[63] thus, the ground state doublet and quartet PESs corresponding to the reactions of silylidyne with singlet and triplet dicarbon, respectively, were calculated. Focusing first on the ground doublet surface, the silicon atom of the silylidyne radical can add without barrier to either carbon atom of the dicarbon molecule producing the silylidyne-ethynyl radical intermediate **D1** (C_2SiH) stabilized by 461 kJ mol^{-1}. From **D1**, there is a low 9 kJ mol^{-1} barrier to cyclization of a CCSi three-membered ring forming **D2**, which can then decompose via atomic hydrogen loss to the cyclic silicon dicarbide molecule (c-SiC_2, **P1**). Alternatively, **D2** may undergo [1,2]-hydrogen shift from the silicon atom to a carbon atom over a 65 kJ mol^{-1} barrier to **D3** before also forming **P1** through hydrogen atom ejection. The only pathways leading to **P2** and **P3** involve ring-opening from **D3** to the linear **D4** intermediate which then unimolecularly decomposes via silicon atom or hydrogen atom loss forming the ethynyl radical (**P2**) and linear silicon dicarbide molecule (**P3**), respectively. However, given the lower energies involved in the dissociations to **P1**, it is expected that its formation will be largely favored.

We now turn our attention to the possibility of reactive collisions occurring in excited electronic states of the compound system (SiC_2H). Given that the silylidyne radical (SiH, $X^2\Pi$) has a doublet multiplicity, its interaction with the singlet dicarbon radical will correlate to two doublet electronic PESs; only the ground state PES can be explored with the highly accurate *ab initio* methods employed here. However, we also know that only one doublet PES (Figure 4) can yield the experimentally detected product **P1**, given that both fragments—SiC_2 (X^1A_1) and atomic hydrogen (^2S)—show nondegenerate electronic states, and that no quartet PES can adiabatically correlate to these products.

Finally, we discuss the reaction of triplet dicarbon ($a^3\Pi_u$) with the doublet silylidyne radical ($X^2\Pi$). The interaction between C_2 ($a^3\Pi_u$) and SiH ($X^2\Pi$) can occur in multiple doublet and quartet states of the compound system (C_2SiH). We note that we cannot exclude that such excited states can contribute to the formation of **P3**. However, as argued above, none of these can yield **P1** adiabatically. To further shed light on the formation of **P2** and **P3**, we present the results of the ground state quartet PES. As the triplet $a^3\Pi_u$ state of dicarbon lies very close in energy to the ground singlet state, the energy of the separated reactants on the ground quartet PES—denoted by red lines in Figure 4—is predicted to be only 8 kJ mol^{-1} above that on the doublet surface, which is in agreement with the reference value for the split between the $X^1\Sigma_g^+$ and

https://doi.org/10.1021/acs.jpclett.6c01640
J. Phys. Chem. Lett. 2026, 17, 9334−9340

$a^3\Pi_u$ states of 8.6 kJ mol^{-1}.[64] Here, the silylidyne radical may add to dicarbon without barrier forming **Q1**, the quartet equivalent of the silylidyne-ethynyl radical (**D1**). Much like the doublet PES, the quartet surface features four intermediates, **Q1**−**Q4**, with isomerization pathways linking them in series, albeit with different energetics. However, decomposition routes to products are distinct from those on the doublet surface, with the available paths **Q1** → **P3**, **Q3** → **P2**, and **Q4** → **P2**. We thoroughly searched for possible seams of crossings between the ground doublet and quartet states; however, none were found, which indicates that intersystem crossings will not contribute to the formation of **P1** from collisions with triplet dicarbon. Thus, the experimentally observed product **P1** must be formed from the reaction of the ground state dicarbon molecule ($X^1\Sigma_g^+$) with the silylidyne radical within the mechanism shown in Figure 4. The simplest and energetically favorable route to **P1** involves just addition, cyclization, and hydrogen atom elimination (**D1** → **D2** → **P1**).

To further shed light on the reactivity of the SiC_2H system, and to compare it with the isovalent C_3H case, frontier molecular orbitals are presented depicting the hydrogen atom ejection to form products (Figure 5). When the hydrogen

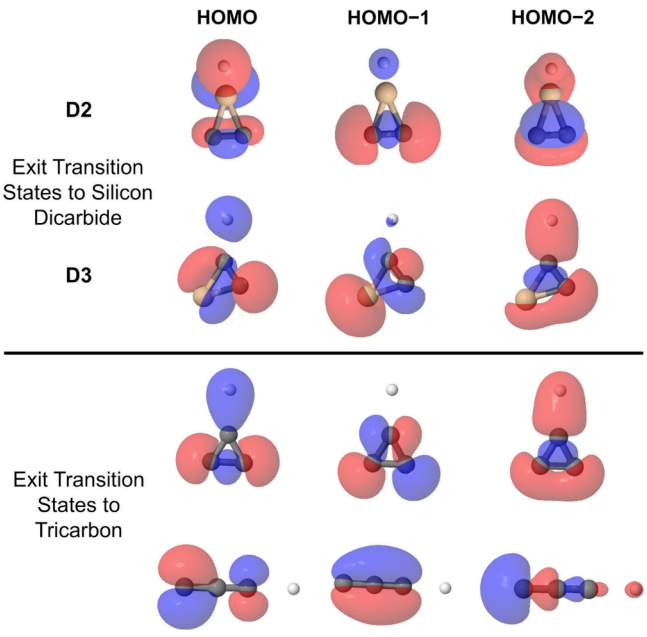

Figure 5. Frontier molecular orbitals for the exit transition states **D2** and **D3** leading to silicon dicarbide, as well as those leading to cyclic and linear tricarbon, via hydrogen atom loss.

atom is removed from **D2**, the highest occupied molecular orbital (HOMO), which contains a single unpaired electron, shows a node in the plane formed by the SiC_2 atoms. This is contrary to what is observed for **D3**, implying that they are composed of different atomic orbitals. Still, comparing the HOMO of these two structures, that of **D2** shows larger intensities around the silicon atom, which is known to be able to expand its valence shell. These two features also occur in the HOMO−2 orbitals of both species. Comparing with the isovalent C_3H system, we first stress that the frontier orbitals of the structure presented in Figure 5 are similar to those of the cyclic C_3H minimum.[65] However, there is a distinct feature of the cyclic C_3H system which does not occur for SiC_2H. Over the course of the hydrogen atom loss at about 150 pm, the singly occupied orbital goes from being the highest in energy (HOMO) to the second highest (HOMO−1). Therefore, in the structure presented in Figure 5, the HOMO−1 has an unpaired electron, and the HOMO is doubly occupied. The singly occupied orbitals in the SiC_2H (HOMO) and C_3H (HOMO−1) systems are similar.

Our crossed molecular beam experiments coupled with high-level electronic structure calculations revealed a barrierless and exoergic route to the cyclic silicon dicarbide molecule (c-SiC_2, X^1A_1, **P1**)—a precursor of silicon carbide grains—via the bimolecular gas-phase reaction of the silylidyne radical (SiH, $X^2\Pi$) with dicarbon (C_2, $X^1\Sigma_g^+$). The reaction proceeds through silylidyne radical center addition to a carbon atom of dicarbon producing the silylidyne-ethynyl intermediate followed by three-membered ring closure and ejection of a hydrogen atom forming cyclic silicon dicarbide. This addition−cyclization−hydrogen-atom-elimination mechanism provides a facile low-temperature pathway initiating the molecular mass growth process of silicon carbide molecules, challenging the current paradigm of silicon carbide formation proceeding only at elevated temperatures. While originally discovered in the circumstellar envelope of the AGB carbon star IRC+10216,[1] more recently the cyclic silicon dicarbide molecule has been observed in the much cooler molecular cloud G+0.693−0.027.[28] This finding suggests the possibility of low-temperature silicon dicarbide formation routes associating astronomical observations with mechanistic laboratory experiments as the key to deciphering the complex organosilicon chemistry in our galaxy.

■ ASSOCIATED CONTENT

Supporting Information

The Supporting Information is available free of charge at https://pubs.acs.org/doi/10.1021/acs.jpclett.6c01640.

Materials and methods, details on the reaction of dicarbon with disilane, laboratory data for the dicarbon−disilane reaction (Figure S1), CM data for the dicarbon−disilane reaction (Figure S2), Cartesian coordinates of all species in the dicarbon−silylidyne reaction (Data S1), supporting references (PDF)

■ AUTHOR INFORMATION

Corresponding Authors

Ralf I. Kaiser − *Department of Chemistry, University of Hawai'i at Mānoa, Honolulu, Hawaii 96822, United States;* orcid.org/0000-0002-7233-7206; Email: ralfk@hawaii.edu

Breno R. L. Galvão − *Centro Federal de Educação Tecnológica de Minas Gerais, 30421-169 Belo Horizonte, MG, Brazil;* orcid.org/0000-0002-4184-2437; Email: brenogalvao@gmail.com

Authors

Shane J. Goettl − *Department of Chemistry, University of Hawai'i at Mānoa, Honolulu, Hawaii 96822, United States;* orcid.org/0000-0003-1796-5725

Iakov A. Medvedkov − *Department of Chemistry, University of Hawai'i at Mānoa, Honolulu, Hawaii 96822, United States;* orcid.org/0000-0003-0672-2090

Zhenghai Yang − *Department of Chemistry, University of Hawai'i at Mānoa, Honolulu, Hawaii 96822, United States*

https://doi.org/10.1021/acs.jpclett.6c01640
J. Phys. Chem. Lett. 2026, 17, 9334−9340

Surajit Metya − *Department of Chemistry, University of Hawai'i at Mānoa, Honolulu, Hawaii 96822, United States;* orcid.org/0009-0004-5583-8481

Márcio O. Alves − *Centro Federal de Educação Tecnológica de Minas Gerais, 30421-169 Belo Horizonte, MG, Brazil*

Complete contact information is available at: https://pubs.acs.org/10.1021/acs.jpclett.6c01640

Notes

The authors declare no competing financial interest.

■ ACKNOWLEDGMENTS

The experimental studies at the University of Hawaii were supported by the US National Science Foundation CHE 2244717. MOA and BRLG thank Conselho Nacional de Desenvolvimento Científico e Tecnológico (CNPq), grant number 305211/2024-2 and Fundação de Apoio à Educação e Desenvolvimento Tecnológico de Minas Gerais (FAPEMIG), grant APQ-02390-25.

■ REFERENCES

(1) Thaddeus, P.; Cummins, S. E.; Linke, R. A. Identification of the SiCC radical toward IRC + 10216: The first molecular ring in an astronomical source. *Astrophys. J.* **1984**, *283*, L45.
(2) Papoular, R.; Cauchetier, M.; Begin, S.; LeCaer, G. Silicon carbide and the 11.3-mu M feature. *Astron. Astrophys.* **1998**, *329*, 1035.
(3) Bernatowicz, T.; Fraundorf, G.; Ming, T.; Anders, E.; Wopenka, B.; Zinner, E.; Fraundorf, P. Evidence for interstellar SiC in the Murray carbonaceous meteorite. *Nature* **1987**, *330*, 728.
(4) Alexander, C. M. O. D.; Swan, P.; Walker, R. M. *In situ* measurement of interstellar silicon carbide in two CM chondrite meteorites. *Nature* **1990**, *348*, 715.
(5) Sarangi, A.; Matsuura, M.; Micelotta, E. R. Dust in supernovae and supernova remnants I: Formation scenarios. *Space Sci. Rev.* **2018**, *214*, 63.
(6) Sloan, G. C.; Matsuura, M.; Zijlstra, A. A.; Lagadec, E.; Groenewegen, M. A. T.; Wood, P. R.; Szyszka, C.; Bernard-Salas, J.; van Loon, J. T. Dust formation in a galaxy with primitive abundances. *Science* **2009**, *323*, 353.
(7) Williams, D. A. Gas and dust in the interstellar medium. *J. Phys.:Conf. Ser.* **2005**, *6*, 1.
(8) Draine, B. T. Interstellar dust grains. *Annu. Rev. Astron. Astrophys.* **2003**, *41*, 241.
(9) Chen, T.; Xiao, C. Y.; Li, A.; Zhou, C. T. Where have all the interstellar silicon carbides gone? *Mon. Not. R. Astron. Soc.* **2021**, *509*, 5231.
(10) Bernal, J. J.; Zega, T. J.; Ziurys, L. M. Destructive processing of silicon carbide grains: Experimental insights into the formation of interstellar fullerenes and carbon nanotubes. *J. Phys. Chem. A* **2022**, *126*, 5761.
(11) Höfner, S.; Olofsson, H. Mass loss of stars on the asymptotic giant branch. *Astron. Astrophys. Rev.* **2018**, *26*, 1.
(12) Agúndez, M.; Martínez, J. I.; de Andres, P. L.; Cernicharo, J.; Martín-Gago, J. A. Chemical equilibrium in AGB atmospheres: Successes, failures, and prospects for small molecules, clusters, and condensates. *Astron. Astrophys.* **2020**, *637*, A59.
(13) Willacy, K.; Cherchneff, I. Silicon and sulphur chemistry in the inner wind of IRC+10216. *Astron. Astrophys.* **1998**, *330*, 676.
(14) Agúndez, M.; Fonfría, J. P.; Cernicharo, J.; Kahane, C.; Daniel, F.; Guélin, M. Molecular abundances in the inner layers of IRC + 10216. *Astron. Astrophys.* **2012**, *543*, A48.
(15) Ziurys, L. M. The chemistry in circumstellar envelopes of evolved stars: Following the origin of the elements to the origin of life. *Proc. Natl. Acad. Sci. U. S. A.* **2006**, *103*, 12274.
(16) Wu, R.; Zhu, C.; Lü, G.; Yang, S.; Meng, Z.; Zhang, X.; Lu, X.; Yu, J.; Chen, W.; Long, M. Dust condensation of SiC, SiO in asymptotic giant branch stellar winds-SiC spectrum. *Res. Astron. Astrophys.* **2024**, *24*, 055002.
(17) Jones, A. P.; Nuth, J. A. Dust destruction in the ISM: A re-evaluation of dust lifetimes. *Astron. Astrophys.* **2011**, *530*, A44.
(18) Dwek, E.; Scalo, J. M. The evolution of refractory interstellar grains in the solar neighborhood. *Astrophys. J.* **1980**, *239*, 193.
(19) Tielens, A. G. G. M. Interstellar depletions and the life cycle of interstellar dust. *Astrophys. J.* **1998**, *499*, 267.
(20) Hutchison, R.; Pillinger, C.; Turner, G.; Russell, S.; Jones, A. P. Interstellar and circumstellar grain formation and survival. *Philos. Trans. R. Soc., A* **2001**, *359*, 1961.
(21) Dwek, E. Iron: A key element for understanding the origin and evolution of interstellar dust. *Astrophys. J.* **2016**, *825*, 136.
(22) Heck, P. R.; Greer, J.; Kööp, L.; Trappitsch, R.; Gyngard, F.; Busemann, H.; Maden, C.; Ávila, J. N.; Davis, A. M.; Wieler, R. Lifetimes of interstellar dust from cosmic ray exposure ages of presolar silicon carbide. *Proc. Natl. Acad. Sci. U. S. A.* **2020**, *117*, 1884.
(23) Kirchschlager, F.; Mattsson, L.; Gent, F. A. Supernova induced processing of interstellar dust: Impact of interstellar medium gas density and gas turbulence. *Mon. Not. R. Astron. Soc.* **2021**, *509*, 3218.
(24) Zhukovska, S.; Dobbs, C.; Jenkins, E. B.; Klessen, R. S. Modeling dust evolution in galaxies with a multiphase, inhomogeneous ISM. *Astrophys. J.* **2016**, *831*, 147.
(25) Michałowski, M. J. Dust production 680−850 million years after the Big Bang. *Astron. Astrophys.* **2015**, *577*, A80.
(26) McKinnon, R.; Torrey, P.; Vogelsberger, M. Dust formation in Milky Way-like galaxies. *Mon. Not. R. Astron. Soc.* **2016**, *457*, 3775.
(27) Massalkhi, S.; Agúndez, M.; Cernicharo, J.; Velilla Prieto, L.; Goicoechea, J. R.; Quintana-Lacaci, G.; Fonfría, J. P.; Alcolea, J.; Bujarrabal, V. Abundance of SiC_2 in carbon star envelopes. *Astron. Astrophys.* **2018**, *611*, A29.
(28) Massalkhi, S.; Jiménez-Serra, I.; Martín-Pintado, J.; Rivilla, V. M.; Colzi, L.; Zeng, S.; Martín, S.; Tercero, B.; de Vicente, P.; Requena-Torres, M. A. The first detection of SiC_2 in the interstellar medium. *Astron. Astrophys.* **2023**, *678*, A45.
(29) Merrill, P. W. Note on the spectrum of UV aurigae. *Publ. Astron. Soc. Pac.* **1926**, *38*, 175.
(30) Sanford, R. F. Two bands in spectra of class N. *Publ. Astron. Soc. Pac.* **1926**, *38*, 177.
(31) Sarre, P. J.; Hurst, M. E.; Lloyd Evans, T. SiC_2 in carbon stars: Merrill-Sanford absorption bands between 4100 and 5500 Å. *Mon. Not. R. Astron. Soc.* **2000**, *319*, 103.
(32) Müller, H. S. P.; Cernicharo, J.; Agúndez, M.; Decin, L.; Encrenaz, P.; Pearson, J. C.; Teyssier, D.; Waters, L. B. F. M. Spectroscopic parameters for silacyclopropynylidene, SiC_2, from extensive astronomical observations toward CW Leo (IRC + 10216) with the Herschel satellite. *J. Mol. Spectrosc.* **2012**, *271*, 50.
(33) McCarthy, M. C.; Gottlieb, C. A.; Thaddeus, P. Silicon molecules in space and in the laboratory. *Mol. Phys.* **2003**, *101*, 697.
(34) Fortenberry, R. C.; Lee, T. J.; Müller, H. S. P. Excited vibrational level rotational constants for SiC_2: A sensitive molecular diagnostic for astrophysical conditions. *Mol. Astrophys.* **2015**, *1*, 13.
(35) Draine, B. T. In *Cosmic Dust - Near and Far*; Henning, T., Grün, E., Steinacker, J., Eds.; 2009; Vol. *414*, p 453.
(36) Smith, I. W. M. General Discussion. *Faraday Discuss.* **2006**, *133*, 228.
(37) Canosa, A.; Le Picard, S. D.; Gougeon, S.; Rebrion-Rowe, C.; Travers, D.; Rowe, B. R. Rate coefficients for the reactions of $Si(^3P_J)$ with C_2H_2 and C_2H_4: Experimental results down to 15 K. *J. Chem. Phys.* **2001**, *115*, 6495.
(38) Kaiser, R. I.; Gu, X. Chemical dynamics of the formation of the ethynylsilylidyne radical ($SiCCH(X^2\Pi)$) in the crossed beam reaction of ground state silicon atoms ($Si(^3P)$) with acetylene ($C_2H_2(X^1\sum_g^+)$). *J. Chem. Phys.* **2009**, *131*, 104311.
(39) Parker, D. S.; Wilson, A. V.; Kaiser, R. I.; Mayhall, N. J.; Head-Gordon, M.; Tielens, A. G. On the Formation of Silacyclopropeny-

lidene (c-SiC_2H_2) and its Role in the Organosilicon Chemistry in the Interstellar Medium. *Astrophys. J.* **2013**, *770*, 33.
(40) Butenhoff, T. J.; Rohlfing, E. A. Laser-induced fluorescence spectroscopy of jet-cooled SiC_2. *J. Chem. Phys.* **1991**, *95*, 1.
(41) Clementi, E.; Kistenmacher, H.; Popkie, H. Study of the electronic structure of molecules. XVIII. Interaction between a lithium atom and a cyano group as an example of a polytopic bond. *J. Chem. Phys.* **1973**, *58*, 2460.
(42) Ross, S. C.; Butenhoff, T. J.; Rohlfing, E. A.; Rohlfing, C. M. SiC_2: A molecular pinwheel. *J. Chem. Phys.* **1994**, *100*, 4110.
(43) Nielsen, I. M. B.; Allen, W. D.; Császár, A. G.; Schaefer, H. F. III Toward resolution of the silicon dicarbide (SiC_2) saga: Ab initio excursions in the web of polytopism. *J. Chem. Phys.* **1997**, *107*, 1195.
(44) Rocha, C. M. R.; Linnartz, H.; Varandas, A. J. C. Reconciling spectroscopy with dynamics in global potential energy surfaces: The case of the astrophysically relevant SiC_2. *J. Chem. Phys.* **2022**, *157*, 104301.
(45) Souza, S. P.; Lutz, B. L. Detection of C_2 in the interstellar spectrum of Cygnus OB2 Number 12 (IV Cygni Number 12). *Astrophys. J.* **1977**, *216*, L49.
(46) Chaffee, F. H., Jr.; Lutz, B. L. The detection of interstellar diatomic carbon toward zeta Ophiuchi. *Astrophys. J.* **1978**, *221*, L91.
(47) Hobbs, L. M. Interstellar C_2 molecules towards zeta Persei. *Astrophys. J.* **1979**, *232*, L175.
(48) Hobbs, L. M. Interstellar C_2 molecules toward OMI Persei. *Astrophys. J.* **1981**, *243*, 485.
(49) van Dishoeck, E. F.; de Zeeuw, T. Observations of interstellar C_2 toward KHI Oph, HD 154368, 147889 and 149404. *Mon. Not. R. Astron. Soc.* **1984**, *206*, 383.
(50) Schilke, P.; Benford, D. J.; Hunter, T. R.; Lis, D. C.; Phillips, T. G. A line survey of Orion-KL from 607 to 725 GHz. *Astrophys. J., Suppl. Ser.* **2001**, *132*, 281.
(51) Goettl, S. J.; Fujioka, K.; Alves, M. O.; Silva, M. X.; Yang, Z.; Metya, S.; Medvedkov, I. A.; Sattasathuchana, T.; Galvão, B. R. L.; Sun, R.; Kaiser, R. I. Gas-phase synthesis of the bicyclic silicon tricarbide molecule (c-SiC_3) as a precursor to silicon carbide nanoparticles in space. *Chem. Sci.* **2026**, *17*, 5367.
(52) Kaiser, R. I.; Ochsenfeld, C.; Stranges, D.; Head-Gordon, M.; Lee, Y. T. Combined crossed molecular beams and ab initio investigation of the formation of carbon-bearing molecules in the interstellar medium via neutral-neutral reactions. *Faraday Discuss.* **1998**, *109*, 183.
(53) Laskin, J.; Lifshitz, C. Kinetic energy release distributions in mass spectrometry. *J. Mass Spectrom.* **2001**, *36*, 459.
(54) Neese, F. Software update: The ORCA program system—Version 5.0. *WIREs Comput. Mol. Sci.* **2022**, *12*, No. e1606.
(55) Grimme, S. Semiempirical hybrid density functional with perturbative second-order correlation. *J. Chem. Phys.* **2006**, *124*, 034108.
(56) Becke, A. D.; Johnson, E. R. A density-functional model of the dispersion interaction. *J. Chem. Phys.* **2005**, *123*, 154101.
(57) Grimme, S.; Ehrlich, S.; Goerigk, L. Effect of the damping function in dispersion corrected density functional theory. *J. Comput. Chem.* **2011**, *32*, 1456.
(58) Weigend, F.; Ahlrichs, R. Balanced basis sets of split valence, triple zeta valence and quadruple zeta valence quality for H to Rn: Design and assessment of accuracy. *Phys. Chem. Chem. Phys.* **2005**, *7*, 3297.
(59) Adler, T. B.; Knizia, G.; Werner, H.-J. A simple and efficient CCSD(T)-F12 approximation. *J. Chem. Phys.* **2007**, *127*, 221106.
(60) Knizia, G.; Adler, T. B.; Werner, H.-J. Simplified CCSD(T)-F12 methods: Theory and benchmarks. *J. Chem. Phys.* **2009**, *130*, 054104.
(61) Dunning, T. H., Jr.; Peterson, K. A.; Wilson, A. K. Gaussian basis sets for use in correlated molecular calculations. X. The atoms aluminum through argon revisited. *J. Chem. Phys.* **2001**, *114*, 9244.
(62) Werner, H. J.; Knowles, P. J.; Knizia, G.; Manby, F. R.; Schütz, M.; Celani, P.; Györffy, W.; Kats, D.; Korona, T.; Lindh, R.; Mitrushenkov, A.; Rauhut, G.; Shamasundar, K. R.; Adler, T. B.; Amos, R. D.; Bernhardsson, A.; Berning, A.; Cooper, D. L.; Deegan, J. O.; Dobbyn, A. J.; Eckert, F.; Goll, E.; Hampel, C.; Hesselmann, A.; Hetzer, G.; Hrenar, T.; Jansen, G.; Köppl, C.; Liu, Y.; Lloyd, A. W.; Mata, R. A.; May, A. J.; McNicholas, S. J.; Meyer, W.; Mura, M. E.; Nicklass, A.; O'Neill, D. P.; Palmieri, P.; Peng, D.; Pflüger, K.; Pitzer, R.; Reiher, M.; Shiozaki, T.; Stoll, H.; Stone, A. J.; Tarroni, R.; Thorsteinsson, T.; Wang, M. *MOLPRO, A Package of Ab Initio Programs*, Version 2015.1; University of Cardiff: Cardiff, UK, 2015; see http://www.molpro.net.
(63) Kaiser, R. I.; Le, T. N.; Nguyen, T. L.; Mebel, A. M.; Balucani, N.; Lee, Y. T.; Stahl, F.; Schleyer, P. v. R.; Schaefer, H. F., III A combined crossed molecular beam and ab initio investigation of C_2 and C_3 elementary reactions with unsaturated hydrocarbons—pathways to hydrogen deficient hydrocarbon radicals in combustion flames. *Faraday Discuss.* **2001**, *119*, 51.
(64) Lias, S. G. In *NIST Chemistry WebBook, NIST Standard Reference Database Number 69*; Linstrom, P. J., Mallard, W. G., Eds.; Institute of Standards and Technology: Gaithersburg, MD.
(65) Bassett, M. K.; Fortenberry, R. C. Symmetry breaking and spectral considerations of the surprisingly floppy c-C_3H radical and the related dipole-bound excited state of c-C_3H^-. *J. Chem. Phys.* **2017**, *146*, 224303.

https://doi.org/10.1021/acs.jpclett.6c01640
J. Phys. Chem. Lett. 2026, 17, 9334−9340